OXFORD

Epigenetic Profiling and Response to CD19 Chimeric Antigen Receptor T-Cell Therapy in B-Cell Malignancies

Carlos A. Garcia-Prieto, MD [ID],[1,2,‡] Lorea Villanueva, PhD [ID],[1,‡] Alberto Bueno-Costa, MSc [ID],[1] Veronica Davalos, PhD [ID],[1] Europa Azucena González-Navarro, PhD,[3] Manel Juan, MD, PhD [ID],[3,4] Álvaro Urbano-Ispizua, MD,[1,4,5] Julio Delgado, MD [ID],[4,6] Valentín Ortiz-Maldonado, MD [ID],[4] Francesca del Bufalo, MD [ID],[7] Franco Locatelli, MD [ID],[7,8] Concetta Quintarelli, MD [ID],[7,9] Matilde Sinibaldi, PhD [ID],[7] Marta Soler, MSc [ID],[1] Manuel Castro de Moura, MSc [ID],[1] Gerardo Ferrer, PhD [ID],[1] Rocio G. Urdinguio, PhD [ID],[10] Agustin F. Fernandez, PhD [ID],[10] Mario F. Fraga, PhD [ID],[10] Diana Bar, BSc,[11] Amilia Meir, MSc,[11] Orit Itzhaki, PhD,[12] Michal J. Besser, PhD,[12,13] Abraham Avigdor, MD,[13,14] Elad Jacoby, MD [ID],[11,13] Manel Esteller, MD, PhD [ID],[1,6,15,16,*]

[1]Cancer and Leukemia Epigenetics and Biology Program (PEBCL), Josep Carreras Leukaemia Research Institute (IJC), Badalona, Spain; [2]Life Sciences Department, Barcelona Supercomputing Center (BSC), Barcelona, Spain; [3]Department of Immunology, Hospital Clinic, Barcelona, Spain; [4]Institut d'Investigacions Biomèdiques August Pi i Sunyer (IDIBAPS), Barcelona, Spain; [5]Department of Hematology, University of Barcelona (UB), Barcelona, Spain; [6]Centro de Investigación Biomédica en Red de Cancer (CIBERONC), Madrid, Spain; [7]Department of Paediatric Haematology and Oncology, Cell and Gene Therapy, Bambino Gesù Children's Hospital, IRCCS, Rome, Italy; [8]Department of Pediatrics, Sapienza University of Rome, Rome, Italy; [9]Department of Clinical Medicine and Surgery, University of Naples Federico II, Naples, Italy; [10]Nanomaterials and Nanotechnology Research Center (CINNCSIC), Health Research Institute of Asturias (ISPA), Institute of Oncology of Asturias (IUOPA), Centro de Investigación Biomédica en Red de Enfermedades Raras (CIBERER), Department of Organisms and Systems Biology (BOS), University of Oviedo, Oviedo, Spain; [11]Division of Pediatric Hematology and Oncology, The Edmond and Lily Safra Children's Hospital, Sheba Medical Center, Tel Hashomer, Ramat Gan, Israel; [12]Ella Lemelbaum Institute for Immuno Oncology, Sheba Medical Center, Tel Hashomer, Ramat Gan, Israel; [13]Sackler School of Medicine, Tel Aviv University, Tel Aviv, Israel; [14]Institute of Hematology, Sheba Medical Center, Tel Hashomer, Ramat Gan, Israel; [15]Institucio Catalana de Recerca i Estudis Avançats (ICREA), Barcelona, Spain; and [16]Physiological Sciences Department, School of Medicine and Health Sciences, University of Barcelona (UB), Spain

‡These authors contributed equally.

*Correspondence to: Manel Esteller, MD, PhD, Josep Carreras Leukaemia Research Institute (IJC), Carretera de Can Ruti, Camí de les Escoles s/n, 08916 Badalona, Barcelona, Catalonia, Spain (e-mail: mesteller@carrerasresearch.org).

ARTICLE

Abstract

Background: Chimeric antigen receptor (CAR) T cells directed against CD19 (CART19) are effective in B-cell malignancies, but little is known about the molecular factors predicting clinical outcome of CART19 therapy. The increasingly recognized relevance of epigenetic changes in cancer immunology prompted us to determine the impact of the DNA methylation profiles of CART19 cells on the clinical course. **Methods:** We recruited 114 patients with B-cell malignancies, comprising 77 patients with acute lymphoblastic leukemia and 37 patients with non-Hodgkin lymphoma who were treated with CART19 cells. Using a comprehensive DNA methylation microarray, we determined the epigenomic changes that occur in the patient T cells upon transduction of the CAR vector. The effects of the identified DNA methylation sites on clinical response, cytokine release syndrome, immune effector cell-associated neurotoxicity syndrome, event-free survival, and overall survival were assessed. All statistical tests were 2-sided. **Results:** We identified 984 genomic sites with differential DNA methylation between CAR-untransduced and CAR-transduced T cells before infusion into the patient. Eighteen of these distinct epigenetic loci were associated with complete response (CR), adjusting by multiple testing. Using the sites linked to CR, an epigenetic signature, referred to hereafter as the EPICART signature, was established in the initial discovery cohort ($n = 79$), which was associated with CR (Fisher exact test, $P < .001$) and enhanced event-free survival (hazard ratio [HR] = 0.36; 95% confidence interval [CI] = 0.19 to 0.70; $P = .002$; log-rank $P = .003$) and overall survival (HR = 0.45; 95% CI = 0.20 to 0.99; $P = .047$; log-rank $P = .04$). Most important, the EPICART profile maintained its clinical course predictive value in the validation cohort ($n = 35$), where it was associated with CR (Fisher exact test, $P < .001$) and enhanced overall survival (HR = 0.31; 95% CI = 0.11 to 0.84; $P = .02$; log-rank $P = .02$). **Conclusions:** We show that the DNA methylation landscape of patient CART19 cells influences the efficacy of the cellular immunotherapy treatment in patients with B-cell malignancy.

Chimeric antigen receptor (CAR) T-cell therapy has proved to be effective in patients for whom few therapeutic options otherwise remain, such as those with relapsed/refractory B-cell acute lymphoblastic leukemia (ALL) and B-cell lymphomas (1-4). These results have led to clinical approval of commercially available treatments (1). Despite the great hopes that CAR T cells directed against CD19 (CART19) cells has raised, treatment failure is not uncommon. The discovery of predictive biomarkers of clinical outcome to CART19 therapy would be highly relevant for risk stratification and the selection of alternative therapies. The lack of initial clinical response or the occurrence of relapse could have several causes related to the CART construct, preparation of infused cells, delivery of transduced cells, and biological features of the targeted B-cells, but only a few defects associated with CART19 inefficacy have been identified, the most studied being tumor antigen escape by loss of the CD19 protein (5). Other candidate molecular biomarkers for predicting CART19 clinical response in preinfused cells include CAR genomic integration sites (6-8) and cytokine expression profiles (9).

Herein, we have addressed whether the epigenetic status of the autologous CAR-transduced T-cells could also affect the clinical course of CART19 therapy. DNA methylation is altered in cancer (10,11), affecting the immune system and immunotherapy efficacy (12). In this regard, DNA methylation signatures are associated with clinical response to programmed cell death protein 1 checkpoint blockade (13) and the DNA methylation status of the vector for transgenic T-cell receptor adoptive cell therapy relates to changes in tumor burden (14). For these reasons, we decided to assess the effects of the DNA methylation landscape of preinfused CART19 cells on the clinical outcome of patients with B-cell malignancies.

Methods

Study Design

Patients were eligible to enter the study if they had an relapsed/refractory B-cell malignancy for which CART19 therapy was recommended. Patient CD19-engineered T cells from 114 cases, comprising 77 patients with ALL and 37 patients with non-Hodgkin lymphoma (NHL), were obtained from 3 academic clinical trials: NCT03144583 (15), NCT02772198 (16,17), and NCT03373071 (18). Written informed consent was obtained, and the Sheba Medical Center institutional review board and the Israeli Ministry of Health, the Research Ethics Committee (Celm) of the Hospital Clinic, and the institutional review board of Bambino Gesù Children Hospital, respectively, provided study approval. The clinical characteristics of the studied 114 patients are summarized in Table 1. The type of CART19 therapy used in each trial is described in Supplementary Methods (available online). High-molecular-weight DNA was extracted from all samples before CART19 infusion into patients.

DNA Methylation Procedure and Analysis

The DNA methylation status of the CART19 cells from each patient was established using the Infinium MethylationEPIC Kit (Illumina, Inc, San Diego, CA) (19). DNA methylation data are available in the Gene Expression Omnibus repository (GSE179414, https://www.ncbi.nlm.nih.gov/geo/query/acc.cgi?acc=GSE179414). An epigenetic signature, referred to hereafter as the EPICART DNA methylation signature (EPICART signature) was obtained using a trained, supervised classification model based on ridge-regularized logistic regression to predict clinical response. The classification model was optimized by tuning parameters (best performance with $\alpha = 0$ from ridge regression and regularization parameter $\lambda = 0.03$), with 10-fold cross-validation, repeated 3 times. Our model performance was assessed using the receiver operating characteristic curve of the resamples (area under the curve mean = 0.83; 95% confidence interval [CI] = 0.75 to 0.91). Flow cytometry analysis was used for validation. DNA methylation status of specific CpG sites was validated by pyrosequencing and bisulfite genomic sequencing of multiple clones. Quantitative reverse transcription–polymerase chain reaction (qRT-PCR) and Western blot were used to assess gene expression (Supplementary Methods; Supplementary Table 1, available online).

Clinical Statistical Analysis

Assay results were compared with patient outcomes in a double-blind manner. The statistical significance of the differences between distributions of the groups was estimated with Fisher exact test. The Mann-Whitney-Wilcoxon test was used to test the statistical significance of the differences between distributions of methylation or expression values among groups. The correlation between methylation and gene expression was estimated using Spearman test. Overrepresentation of T-cell population phenotypes in EPICART-positive and EPICART-negative CART19 cells was estimated using the Student t test. Event-free survival (EFS) was defined as the time from the start of CART19 treatment until the first occurrence of progression, relapse, or death. Overall survival (OS) was defined as the time from the start of CART19 treatment until death. The Kaplan-Meier method was also used to estimate the EFS and OS, the differences between the groups being calculated with the log-rank test. Hazard ratios from univariate Cox regressions were used to determine the association between clinicopathological features and survival. A P value less than 0.05 was considered statistically significant. All statistical tests were 2-sided unless otherwise stated.

Results

The Epigenomic Landscape of CART19 Cells

To discover an epigenomic profile associated with patients with a B-cell malignancy who would gain clinical benefit from CART19 treatment, we first studied the DNA methylation landscape of untransduced and transduced preinfusion T cells for the CD19 CAR retrovirus in 43 patients from the NCT02772198 clinical trial (Figure 1, A). This set of cases included 30 NHL (28 adult and 2 pediatric patients) and 13 ALL (8 pediatric and 5 adult patients). In this initial set, we interrogated the methylation status of approximately 850 000 CpG sites (19). In the 43 patients with a B-cell malignancy, DNA methylation levels differed between CART19 untransduced and transduced cells at 984 CpG sites (Supplementary Table 2, available online). Among these differential CpG sites, 52.7% (519 of 984) were

Table 1. Clinicopathological characteristics of the patients with a B-cell malignancy treated with chimeric antigen receptor T cells directed against CD19 cells[a]

Characteristic	Entire cohort (n = 114)	Discovery cohort (n = 79)	Validation cohort (n = 35)
Sex, No. (%)			
Male	68 (59.6)	41 (51.9)	27 (77.1)
Female	46 (40.4)	38 (48.1)	8 (22.9)
Median age (range), y	24 (3-70)	22 (3-70)	27 (4-70)
Age, No. (%), y			
<18	42 (36.8)	32 (40.5)	10 (28.6)
18-29	27 (23.7)	16 (20.3)	11 (31.4)
30-59	34 (29.8)	26 (32.9)	8 (22.9)
≥60	11 (9.6)	5 (6.3)	6 (17.1)
Diagnosis, No. (%)			
B-ALL	77 (67.5)	53 (67.1)	24 (68.6)
B-NHL	37 (32.5)	26 (32.9)	11 (31.4)
DLBCL	20 (17.5)	13 (16.5)	7 (20.0)
PMBCL	11 (9.6)	9 (11.4)	2 (5.7)
Follicular lymphoma	4 (3.5)	3 (3.8)	1 (2.9)
Burkitt lymphoma	1 (0.9)	0 (0.0)	1 (2.9)
Mantle cell lymphoma	1 (0.9)	1 (1.3)	0 (0.0)
Response, No. (%)			
CR	74 (64.9)	50 (63.3)	24 (68.6)
PR	16 (14)	11 (13.9)	5 (14.3)
Stable disease	9 (7.9)	6 (7.6)	3 (8.6)
Disease progression	15 (13.2)	12 (15.2)	3 (8.6)
CRS, No. (%)			
Grade 0	41 (36.0)	28 (35.4)	13 (37.1)
Grade 1	46 (40.4)	33 (41.8)	13 (37.1)
Grade 2	13 (11.4)	10 (12.7)	3 (8.6)
Grade 3	8 (7.0)	4 (5.1)	4 (11.4)
Grade 4	4 (3.5)	2 (2.5)	2 (5.7)
Grade 5	2 (1.8)	2 (2.5)	0 (0.0)
ICANS, No. (%)			
Grade 0	87 (76.3)	59 (74.7)	28 (80.0)
Grade 1	11 (9.6)	8 (10.1)	3 (8.6)
Grade 2	5 (4.4)	4 (5.1)	1 (2.9)
Grade 3	6 (5.3)	4 (5.1)	2 (5.7)
Grade 4	5 (4.4)	4 (5.1)	1 (2.9)
Grade 5	0 (0.0)	0 (0.0)	0 (0.0)
Origin of the CAR T cells			
NCT02772198	43 (37.7)	30 (38.0)	13 (37.1)
NCT03144583	45 (39.5)	31 (39.2)	14 (40.0)
NCT03373071	26 (22.8)	18 (22.8)	8 (22.9)

[a]B-ALL = B-cell acute lymphoblastic leukemia; B-NHL = B-cell non-Hodgkin lymphoma; CAR = chimeric antigen receptor; CR = complete response; CRS = cytokine release syndrome; DLBCL = diffuse large B-cell lymphoma; ICANS = immune effector cell-associated neurotoxicity syndrome; PMBCL = primary mediastinal B-cell lymphoma; PR = partial response.

hypermethylation events at the CART19 transduced cells vs the untransduced cells, whereas 47.3% (465 of 984) were hypomethylation changes. The CpG methylation content of these 984 sites was not distinct between CD4 and CD8 T cells (CD4 methylation β value 95% CI = 0.57 to 0.61; CD8 methylation β value 95% CI = 0.57 to 0.61, Mann-Whitney-Wilcoxon test $P = .73$). The genomic distribution of these CpG sites is illustrated in Figure 1, B. They were associated with known genes in 75.1% (739 of 984) of cases and, of these, were located within a defined regulatory region in 45.9% (339 of 739) of cases. Gene set enrichment analysis using gene ontology collections showed that the most overrepresented biological processes and Kyoto Encyclopedia of Genes and Genomes and Reactome pathways were the "T-cell receptor signaling pathway," "Pathways in cancer," and "Separation of sister chromatids," respectively (Figure 1, C).

Using only CpG sites for regulatory regions, the most overrepresented categories were "T-cell receptor signaling pathway" and "Transcriptional regulation by RUNX3" (Supplementary Figure 1, A, available online), whereas using only gene body sites, the most overrepresented categories were "Homophilic cell adhesion via plasma membrane adhesion molecules" and "Separation of sister chromatids" (Supplementary Figure 1, B, available online).

T cells transduced with CD19 CAR retroviruses could themselves be vulnerable to DNA methylation silencing (20). Thus, we examined whether a distinct DNA methylation status of the retrovirus in the transduced T-cell could also influence clinical outcome. Pyrosequencing analyses of the retroviral vector showed an unmethylated status of the retroviral vector in the CART19 cells (Supplementary Figure 1, C, available online).
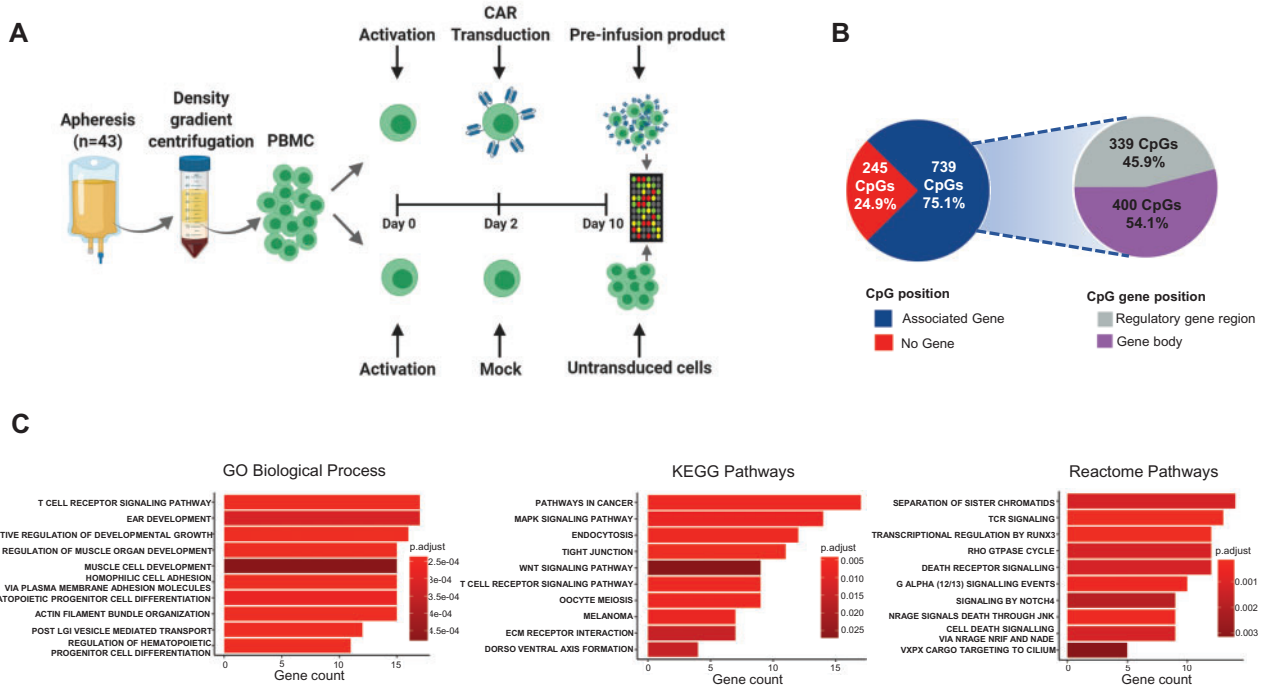
Figure 1. Characterization of epigenetic changes in patient T cells upon transduction of the chimeric antigen receptor (CAR) vector. **A)** Experimental design developed to detect DNA methylation changes in patient T cells upon CAR transduction. **B)** Distribution of the 984 CpG sites identified in the human genome. **C)** Gene ontology (GO) analysis of genes with CpGs that changed upon CAR transduction (overrepresentation analysis with false discovery rate adjusted $P < .05$). KEGG = Kyoto Encyclopedia of Genes and Genomes; PBMC = Peripherla Blood Mononuclear Cell.

Impact of CART19 Epigenetics in Clinical Outcome: The EPICART Signature

Fisher exact test with correction for multiple hypothesis testing using the false discovery rate (FDR) was applied to identify any association between the DNA methylation status of the 984 CpG sites identified in CART19-transduced cells and the clinical outcomes in 114 patients with a B-cell malignancy treated with this type of cell therapy (Table 1). For the contingency tables, clinical response was categorized as complete response (CR) vs non-CR (partial response + stable disease + disease progression). For the adverse effects, we followed the guidelines of the American Society for Transplantation and Cellular Therapy (21): Cytokine release syndrome (CRS) was divided into grade 0 vs grades 1 through 5, and immune effector cell-associated neurotoxicity syndrome (ICANS) was split into grade 0 vs grades 1 through 5. These cases were divided into a discovery cohort of 79 patients and a validation cohort of 35 patients (Table 1). The 2 cohorts did not show statistically significant differences related to age (pediatric vs adult; Fisher exact test, $P = .29$), origin of the sample (NCT03144583, NCT02772198, and NCT03373071; Fisher exact test, $P = 1$), type of B-cell malignancy (ALL vs NHL; Fisher exact test, $P = 1$), clinical response (CR vs partial response, stable disease, or disease progression; Fisher exact test, $P = .67$), or the appearance of CRS (0 vs 1-5; Fisher exact test, $P = 1$) or ICANS (0 vs 1-5; Fisher exact test, $P = .64$). DNA from the CART19-transduced cells infused in each patient was hybridized to the described DNA methylation microarray (19).

In our discovery cohort ($n = 79$), we found 54 CpG sites (5.5% of the 984 sites) at the initial screening by Fisher exact test for which the DNA methylation levels were statistically

significantly associated with clinical variables. The DNA methylation status of 45, 8, and 5 CpG sites was associated, respectively, with CR (Supplementary Table 3, available online), CRS (Supplementary Table 4, available online), and ICANS (Supplementary Table 5, available online). We then applied to all the identified CpG sites with potential clinical value derived from the Fisher exact test the FDR statistical approach used in multiple-hypothesis testing to correct for multiple comparisons. We found that although the epigenetic loci linked to CRS and ICANS failed this test, 40.0% (18 of 45) of the CpG sites associated with CR passed the FDR for multiple testing (Supplementary Table 6, available online).

When we had established that a set of 18 epigenomic loci adjusted by multiple testing could discriminate a CR result following CART19 treatment (Supplementary Table 6, available online), we examined whether these sites could also predict EFS and OS in our discovery cohort ($n = 79$). In this regard, the presence of a CR was associated with enhanced EFS and improved OS (Figure 2, A). When we selected the 18 methylation sites associated with CR (Supplementary Table 6, available online) to train a supervised classification model based on ridge-regularized logistic regression, we obtained an EPICART signature. The use of the EPICART signature in the supervised hierarchical clustering for the discovery cohort of CART cases classified patients as those exhibiting CR or non-CR (Fisher exact test, $P < .001$) (Supplementary Figure 2, available online). Most important, the EPICART signature was associated with EFS (Figure 2, B) and OS (Figure 2, B).

Taking advantage of the dissected DNA methylation patterns of the different T-cell populations from the International Human Epigenome Consortium (22), we undertook a molecular
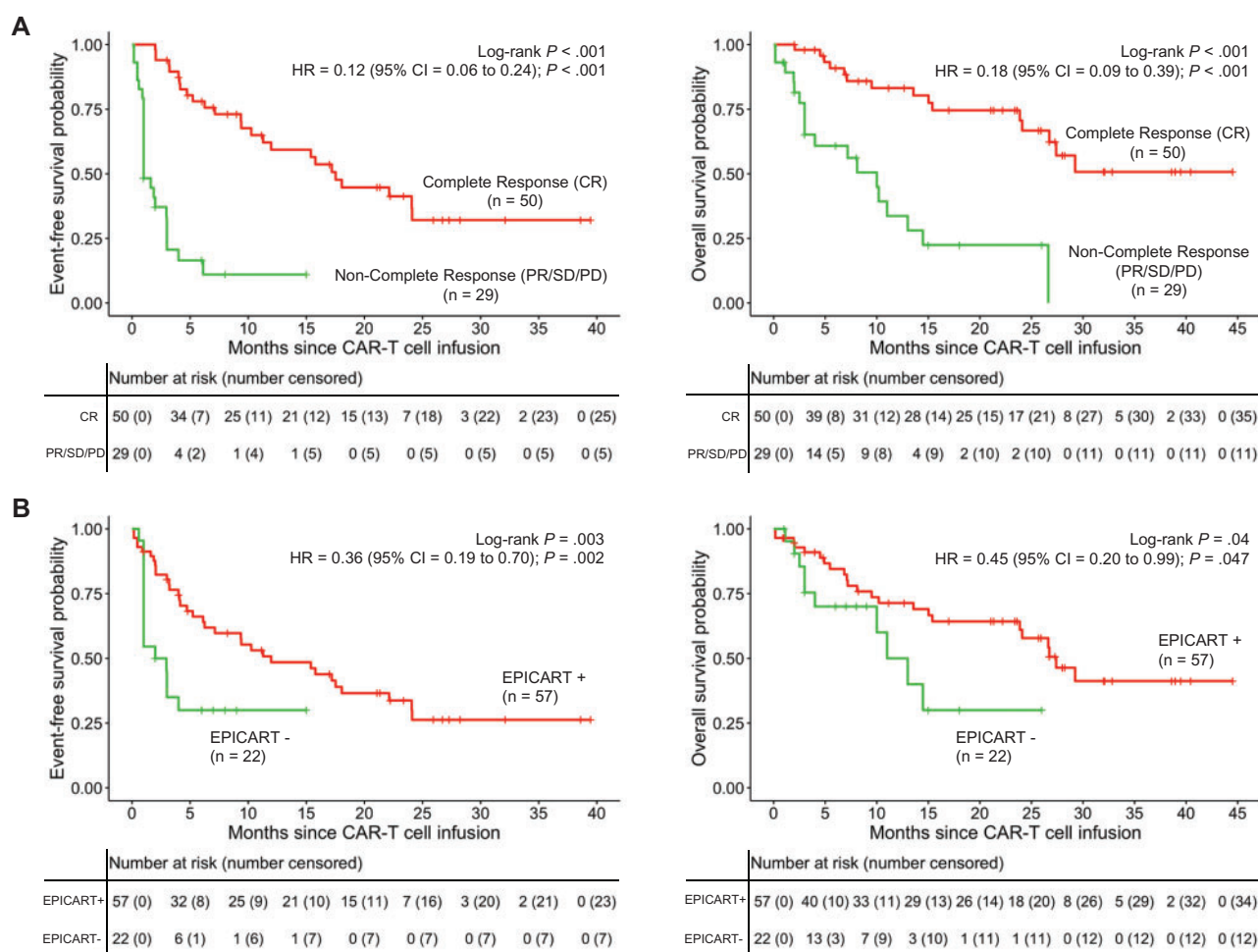
Figure 2. Complete response (CR) and DNA methylation signature (EPICART) associated with event-free survival (EFS) and overall survival (OS) in the discovery cohort of patients with a B-cell malignancy treated with chimeric antigen receptor T cells directed against CD19 (CART19) therapy. **A)** Kaplan-Meier analysis of EFS (left) and OS (right) in 79 patients with a B-cell malignancy according to the presence of CR or its absence (partial response [PR] + stable disease [SD] + progression of the disease [PD]). **B)** Kaplan-Meier analysis of EFS (left) and OS (right) in the same patients with a B-cell malignancy according to the presence of an EPICART signature in the preinfused CART19 cells, defined by the methylation status of the 18 CpG sites associated with CR (EPICART-positive [+] signature). For all cases, the P value was calculated using the log-rank function. Univariate Cox regression analysis is represented as the hazard ratio (HR), with a 95% confidence interval (CI). A P value less than .05 was considered statistically significant. The number of events is also shown. All statistical tests were 2-sided.

dissection of the T-cell classes in our EPICART signature. We found that the EPICART-positive signature identified CART19 cells enriched in CD4 and CD8 naive-like or early memory phenotype T cells (Fisher exact test, $P = .03$). Conversely, EPICART-negative CART19 cells were enriched in more committed and differentiated lineages, such as effector memory CD4 and CD8 T cells, and terminally differentiated effector memory CD8 T cells (Fisher exact test, $P < .001$). The described population phenotypes assigned by computational projection were validated by flow cytometry analyses in 43 cases (38 ALL and 5 NHL) of the discovery cohort, where these data were available. The use of the markers CD3, CD45RA, and CCR7 to define the population status of naive T cells (TNs: CD3+CD45RA+CCR7+), central memory T cells (TCMs: CD3+CD45RA-CCR7+), effector memory T cells (CD3+CD45RA-CCR7−), and effector T cells (TEMRAs: CD3+CD45RA+CCR7−) confirmed that EPICART-positive CART19 cells were enriched in TNs/central TCMs (EPICART-positive cells, 95% CI = 48.39% to 66.17%; EPICART-negative cells, 95% CI = 20.13% to 56.19%; Student *t* test, $P = .04$), whereas in EPICART-negative cells effector memory T-cell/TEMRA

populations were overrepresented (EPICART-positive cells, 95% CI = 28.31% to 45.63%; EPICART-negative cells, 95% CI = 39.86% to 75.24%; Student *t* test, $P = .03$) (Supplementary Methods, available online). Examples of flow cytometry analyses are shown in Supplementary Figure 3, A (available online). Importantly, we observed that those patients with a B-cell malignancy receiving CARTs enriched with TN + TCM showed improved EFS and OS compared with those given adoptive cell therapy enriched with effector memory T cell + TEMRA (Supplementary Figure 3, B, available online). These results are consistent with the adoptive cell therapy concept that TNs or early TCMs can outperform TEMRAs because of the limited niche homing, survival, and self-renewal capacity of the effector cells relative to the less committed and more immature T cells (23-27).

Related to any obvious impact on gene expression for the 18 CpG sites that defined the EPICART signature, RNA or protein for the CART19 cells was not available; thus, we data-mined 100 blood cell lines analyzed for DNA methylation and expression (28). We observed that hypermethylation of those CpG sites
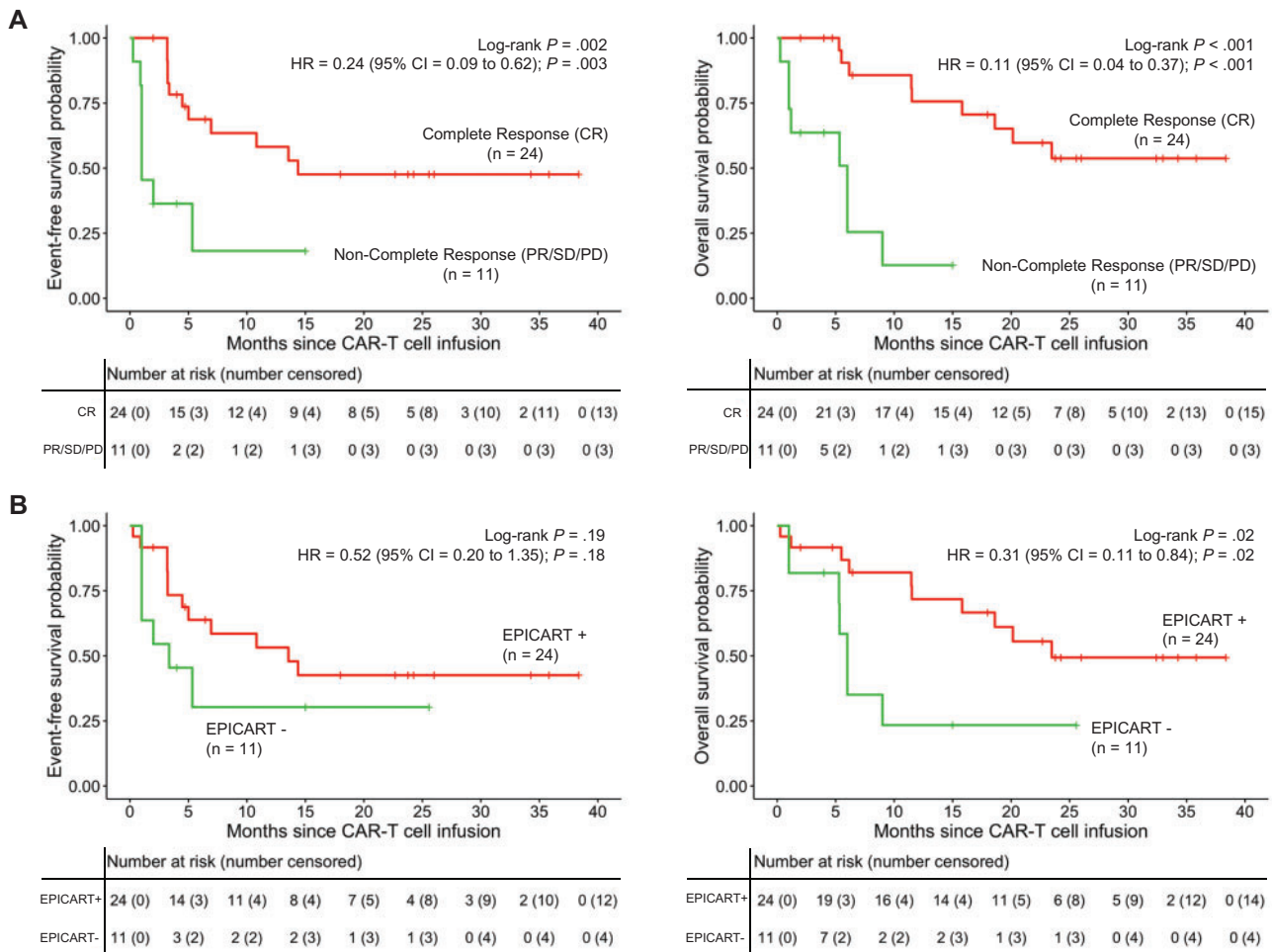
Figure 3. Complete response (CR) and DNA methylation (EPICART) signature associated with event-free survival (EFS) and overall survival (OS) in the validation cohort of patients with a B-cell malignancy treated with chimeric antigen receptor T cells directed against CD19 (CART19) therapy. **A)** Kaplan-Meier analysis of EFS (left) and OS (right) in 35 patients with a B-cell malignancy according to the presence of CR or its absence (partial response [PR] + stable disease [SD] + progression of the disease [PD]). **B)** Kaplan-Meier analysis of EFS (left) and OS (right) in the same patients with a B-cell malignancy according to the presence EPICART signature in the preinfused CART19 cells, defined by the methylation status of the 18 CpG sites associated with CR (EPICART-positive [+] signature). For all cases, the P value was calculated using the log-rank function. Univariate Cox regression analysis is represented as the hazard ratio (HR) with a 95% confidence interval (CI). A P value less than .05 was considered statistically significant. The number of events is also shown. All statistical tests were 2-sided.

located in the gene bodies was associated with transcript upregulation (methylated CpGs z score, 95% CI = 0.30 to 0.49; unmethylated CpGs z score, 95% CI = −0.28 to −0.02; Mann-Whitney-Wilcoxon test, $P < .001$) (Supplementary Figure 4, A, available online). Illustrative examples are shown for the hypermethylated CpG sites in the gene bodies of INPP5A and ECHDC1 (Supplementary Table 6, available online) (Spearman test in 100 blood cell lines, $\rho > 0.3$; $P < .001$) (Supplementary Figure 4, B, available online). The presence of gene body hypermethylation accompanied by gene upregulation has been reported (29). Importantly, using T-cell–derived lines from these analyses, we validated that INPP5A and ECHDC1 gene-body hypermethylation was associated with elevated expression, whereas gene-body hypomethylation was associated with gene downregulation (Supplementary Figure 4, C, available online). Concordantly, the use of the DNA methylation inhibitor 5-Aza-2'-deoxycytidine in the hypermethylated cell lines downregulated INPP5A and ECHDC1 expression (Supplementary Figure 4, D, available online). Furthermore, we experimentally validated by pyrosequencing and bisulfite genomic sequencing of multiple clones

the DNA methylation status of these CpG sites in EPICART-positive and negative patients (Supplementary Figure 4, E, available online). Further data mining of the T-cell–derived lines showed that hypermethylation of 5'-end CpG sites was statistically significantly associated with transcript downregulation (Supplementary Figure 4, F, available online). An illustrative example is the 5'-UTR CpG hypermethylation of FOXN3, a candidate tumor suppressor for T-cell ALL (30) (Supplementary Figure 4, G, available online).

EPICART Validation and Single Loci Associated With Clinical Course

Having characterized the EPICART signature as being a predictor of CR, EFS, and OS in the discovery cohort of B-cell malignancies treated with CART19, we asked whether the identified DNA methylation landscape could also distinguish clinical outcome in the validation cohort (Table 1). From a clinical standpoint, CR was associated with enhanced EFS and improved OS in the

Table 2. Annotation of the 6 CpGs correlated with complete response and with statistically significant improvement in event-free survival and overall survival[a]

Probe ID[b]	Chromosomal position (hg19)[c]	Associated gene[d]	CR FDR P value[e]	EFS P value[f]	OS P value[f]
cg12012941	chr1:188676237	Not described	<.001	.01	.01
cg04267686	chr6:105907265	Not described	.001	.02	.001
cg25534076	chr1:234087867	SLC35F3	.002	.04	.03
cg12260379	chr2:86332162	PTCD3; POLR1A	.01	.03	.04
cg09992216	chr11:32353565	Not described	.01	.009	.004
cg12610471	chr10:22634199	SPAG6	.02	.001	.003

[a]Annotation retrieved from the Infinium MethylationEPIC Array Kit (Illumina, Inc, San Diego, CA) manifest. CR = complete response; EFS = event-free survival; FDR = false discovery rate; OS = overall survival.
[b]Unique identifier from the Illumina CpG database.
[c]Chromosomal coordinates of the CpG (build hg19).
[d]Target gene name from the University of California Santa Cruz database.
[e]The FDR-adjusted P value of the CR is derived from the Fisher exact test (CR vs no response/stable disease/disease progression). All tests were 2-sided.
[f]The P value of EFS and OS is derived from the log-rank test in Kaplan-Meier curves. All tests were 2-sided.
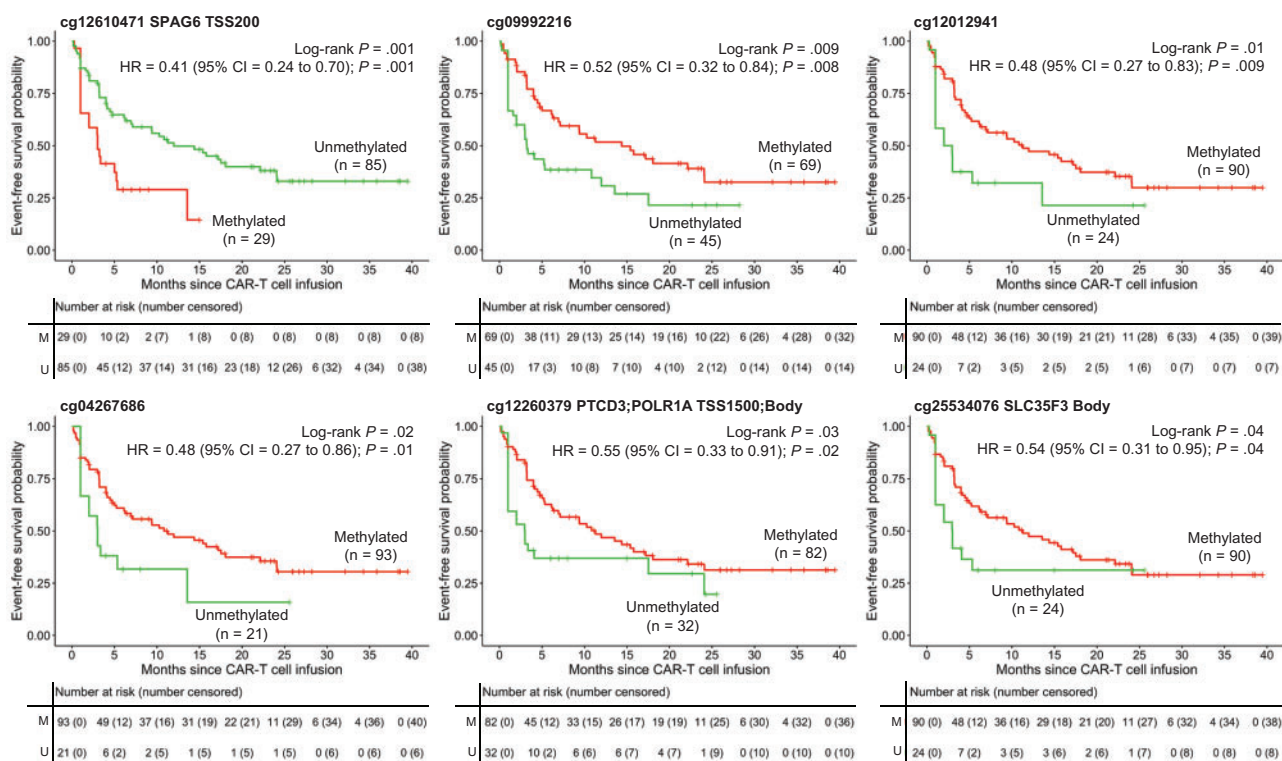

Figure 4. Kaplan-Meier estimates of event-free survival with respect to the chimeric antigen receptor T cells directed against CD19 (CART19) cell preinfusion methylation status of 6 candidate single CpG loci in patients with a B-cell malignancy treated with the adoptive cell therapy. The P value was calculated using the log-rank function. Univariate Cox regression analysis is represented as the hazard ratio (HR) with a 95% confidence interval (CI). A P value of less than .05 was considered statistically significant. The number of events is also shown. All statistical tests were 2-sided. M = methylated; U = unmethylated.

validation set (Figure 3, A). Importantly, EPICART signature predicted CR to CART cell therapy with 82.9% accuracy (95% CI = 66.4% to 93.4%; κ = 0.60), 87.5% sensitivity, and 72.7% specificity in the validation cohort. We further evaluated the model performance using the receiver operating characteristic curve, obtaining an area under the curve value of 0.80. Use of the EPICART signature in the supervised hierarchical clustering for the validation cohort of CART cases also distinguished CR or non-CR (Fisher exact test, P < .001) (Supplementary Figure 5, A, available online). Remarkably, the EPICART-positive signature

was associated with improved OS in the validation cohort (hazard ratio = 0.31; 95% CI = 0.11 to 0.84; P = .02; log-rank P = .02) (Figure 3, B). We also found a nonstatistically significant trend between the EPICART-positive signature and EFS (hazard ratio = 0.52; 95% CI = 0.20 to 1.35; P = .18; log-rank P = .19) (Figure 3, B).

Finally, for the entire cohort, CR was associated with EFS and OS (Supplementary Figure 5, B, available online). The EPICART signature in the supervised hierarchical clustering for the complete set of available cases (discovery + validation, n = 114) also
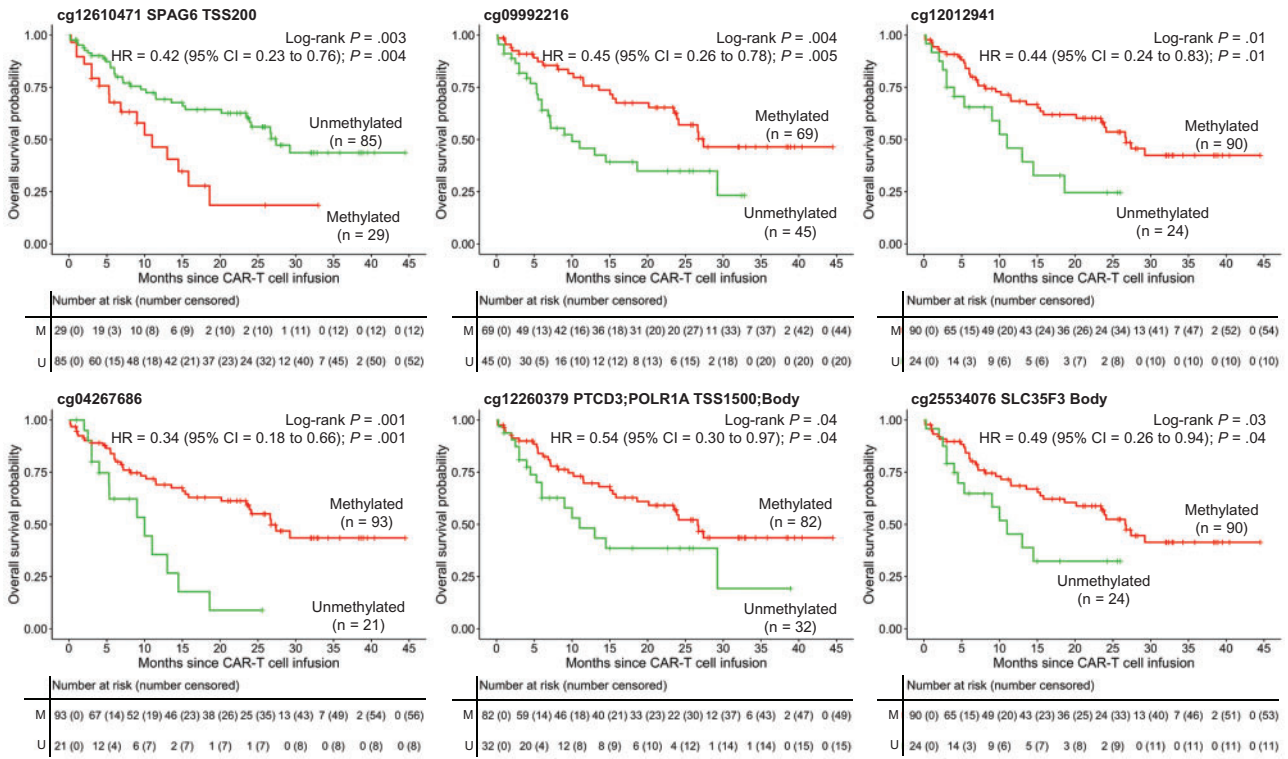
ARTICLE

Figure 5. Kaplan-Meier estimates of overall survival relative to the chimeric antigen receptor T cells directed against CD19 (CART19) cell preinfusion methylation status of 6 candidate single CpG loci in patients with a B-cell malignancy treated with adoptive cell therapy. The *P* value was calculated using the log-rank function. Univariate Cox regression analysis is represented as the hazard ratio (HR) with a 95% confidence interval (CI). A *P* value of less than .05 was considered statistically significant. The number of events is also shown. All statistical tests were 2-sided. M = methylated; U = unmethylated.

classified patients as those exhibiting CR or non-CR (Fisher exact test, P < .001) (Supplementary Figure 5, C, available online). Importantly, in the entire cohort, EPICART-positive signature was associated with improved EFS and OS (Supplementary Figure 5, D, available online). The hazard ratios and P values for EFS and OS obtained from each cohort are summarized in Supplementary Table 7 (available online).

To identify a smaller set of biomarkers that could simplify the analysis, we found 6 epigenomic loci from the EPICART signature that, analyzed alone, were also associated with improved EFS and OS. These CpG sites are summarized in Table 2, and the corresponding Kaplan-Meier curves for EFS and OS are shown in Figures 4 and 5, respectively. The 4 genes associated with these 6 DNA methylation loci were PTCD3 and POLR1A, involved in protein production regulation at ribosomes (31,32); SLC35F3, a thiamine transferase involved in T-cell infiltration (33); and SPAG6, which regulates cell apoptosis through tumor necrosis factor–related apoptosis-inducing ligand (TRAIL) signaling (34). SPAG6 was further studied, given the proposed used of a TRAIL variant to overcome CART resistance (35) and the CpG location at the transcription start site. We observed in T-cell–derived lines the association between SPAG6 hypermethylation and downregulation measured by qRT-PCR and Western blot (Supplementary Figure 6, A and B, available online). Hypermethylation-associated silencing was also found for PTCD3, the other candidate gene with an identified differentially methylated CpG site in its promoter region (Supplementary Figure 6, C and D, available online).

Discussion

The use of CART19 therapy has improved the clinical outcome of patients with relapsed/refractory B-cell malignancies (1-4). Despite the promising initial results, however, a not-negligible proportion of cases does not show CR or does not achieve long-term remission (1-4). This finding is relevant from the point of view of patient care because this therapy may be accompanied by some serious side effects, such as CRS and ICANS, and also from the health provider standpoint because it is an expensive therapy. Thus, it would be helpful to identify biomarkers associated with CART19 clinical outcomes. Our study shows that the epigenetic profiling in CAR19-transduced T lymphocytes provides a consistent readout associated with clinical outcomes.

Our findings indicate that the intrinsic molecular features of the preinfusion cells determine the success of the adoptive cell therapy. In this regard, global RNA expression patterns of the preinfused T-cell differs between CR and non-CR patients (6), an observation added to the impact on outcome of the CAR integration site (8). All these findings support the finding that the "fitness" of preinfused CART19 cells contributes to treatment effectiveness. In this regard, CART19 cell products that harbor particular T-cell subsets are more clinically effective (6). Differences in the conditions of the manufacturing process from commercially available treatments and the unique functional background of the transduced T cells of each patient can modify the "omics" landscape of preinfused cells, directly affecting their activity. Importantly, it has recently been reported that epigenetic remodeling can restore functionality in

exhausted CART cells ([36](36)), further supporting the impact of these changes.

Our results strengthen the notion that the molecular profiles of the cells used in adoptive cell therapy is of great value for determining treatment success. This approach has also been proposed for immune checkpoint inhibitors ([13,14](13,14)). Thus, biomarkers of the efficacy of adoptive cell therapy, similar to those cited here ([5-9,37](5-9,37)), and the DNA methylation markers discovered in our study almost certainly await discovery. Two examples highlight the potential of studies in this area. One is the occurrence of T-cell receptor epigenetic inactivation associated with reduced tumor responsiveness in patients with melanoma and sarcoma infused with autologous T cells transduced with a retrovirus ([14](14)). Importantly, US Food and Drug Administration–approved CART19 treatments with axicabtagene ciloleucel and brexucabtagene autoleucel use retroviruses. A second pertinent study used single-cell RNA sequencing, a technique recently applied for CAR T cells ([38](38)), to show that mural cells, which surround the endothelium maintaining bloodbrain barrier integrity, express the CD19 antigen ([39](39)), which may explain the neurotoxicity observed in CART19 therapies ([40](40)).

Overall, we report that the DNA methylation landscape of preinfusion CART19 cells can predict which patients with a B-cell malignancy will gain a clinical benefit. Importantly for its proposed clinical use, the best of the candidate sites identified within our epigenomic signature could be assessed using single PCR-based assays. In this regard, although larger, prospective clinical studies are required to determine the final value of the DNA methylation loci identified here, assessing the epigenetic profile of the CAR19-transduced, preinfused T cells could help solve the unmet medical need to identify patients who would benefit the most from CAR T-cell therapy.

Funding

Notes

Data Availability

All relevant data are shown in the main manuscript and the Supplementary Materials. DNA methylation data are available in the Gene Expression Omnibus repository (GSE179414, https://www.ncbi.nlm.nih.gov/geo/query/acc.cgi?acc=GSE179414).

References

1. Elsallab M, Levine BL, Wayne AS, Abou-El-Enein M . CAR T-cell product performance in haematological malignancies before and after marketing authorisation. *Lancet Oncol.* 2020;21(2):e104–e116.
2. Singh AK, McGuirk JP. CAR T cells: continuation in a revolution of immunotherapy. *Lancet Oncol.* 2020;21(3):e168–e178.
3. Kersten MJ, Spanjaart AM, Thieblemont C. CD19-directed CAR T-cell therapy in B-cell NHL. *Curr Opin Oncol.* 2020;32(5):408–417.
4. Malard F, Mohty M. Acute lymphoblastic leukaemia. *Lancet.* 2020;395(10230):1146–1162.
5. Majzner RG, Mackall CL. Tumor antigen escape from CAR T-cell therapy. *Cancer Discov.* 2018;8(10):1219–1226.
6. Fraietta JA, Lacey SF, Orlando EJ, et al. Determinants of response and resistance to CD19 chimeric antigen receptor (CAR) T cell therapy of chronic lymphocytic leukemia. *Nat Med.* 2018;24(5):563–571.
7. Fraietta JA, Nobles CL, Sammons MA, et al. Disruption of TET2 promotes the therapeutic efficacy of CD19-targeted T cells. *Nature.* 2018;558(7709):307–312.
8. Nobles CL, Sherrill-Mix S, Everett JK, et al. CD19-targeting CAR T cell immunotherapy outcomes correlate with genomic modification by vector integration. *J Clin Invest.* 2020;130(2):673–685.
9. Rossi J, Paczkowski P, Shen YW, et al. Preinfusion polyfunctional anti-CD19 chimeric antigen receptor T cells are associated with clinical outcomes in NHL. *Blood.* 2018;132(8):804–814.
10. Berdasco M, Esteller M. Clinical epigenetics: seizing opportunities for translation. *Nat Rev Genet.* 2019;20(2):109–127.
11. Moran S, Martínez-Cardús A, Sayols S, et al. Epigenetic profiling to classify cancer of unknown primary: a multicentre, retrospective analysis. *Lancet Oncol.* 2016;17(10):1386–1395.
12. Villanueva L, Álvarez-Errico D, Esteller M. The contribution of epigenetics to cancer immunotherapy. *Trends Immunol.* 2020;41(8):676–691.
13. Duruisseaux M, Martínez-Cardús A, Calleja-Cervantes ME, et al. Epigenetic prediction of response to anti-PD-1 treatment in non-small-cell lung cancer: a multicentre, retrospective analysis. *Lancet Respir Med.* 2018;6(10):771–781.
14. Nowicki TS, Farrell C, Morselli M, et al. Epigenetic suppression of transgenic T-cell receptor expression via gamma-retroviral vector methylation in adoptive cell transfer therapy. *Cancer Discov.* 2020;10(11):1645–1653.
15. Ortíz-Maldonado V, Rives S, Castellà M, et al. CART19-BE-01: a multicenter trial of ARI-0001 cell therapy in patients with CD19+ relapsed/refractory malignancies. *Mol Ther.* 2021;29(2):636–644.
16. Jacoby E, Bielorai B, Avigdor A, et al. Locally produced CD19 CAR T cells leading to clinical remissions in medullary and extramedullary relapsed acute lymphoblastic leukemia. *Am J Hematol.* 2018;93(12):1485–1492.
17. Itzhaki O, Jacoby E, Nissani A, et al. Head-to-head comparison of in-house produced CD19 CAR-T cell in ALL and NHL patients. *J Immunother Cancer.* 2020;8(1):e000148.
18. Quintarelli C, Guercio M, Manni S, et al. Strategy to prevent epitope masking in CAR.CD19+ B-cell leukemia blasts. *J. Immunother. Cancer.* 2021;9(6):e001514.
19. Moran S, Arribas C, Esteller M. Validation of a DNA methylation microarray for 850,000 CpG sites of the human genome enriched in enhancer sequences. *Epigenomics.* 2016;8(3):389–399.
20. Yao S, Sukonnik T, Kean T, Bharadwaj RR, Pasceri P, Ellis J. Retrovirus silencing, variegation, extinction, and memory are controlled by a dynamic interplay of multiple epigenetic modifications. *Mol Ther.* 2004;10(1):27–36.
21. Lee DW, Santomasso BD, Locke FL, et al. ASTCT consensus grading for cytokine release syndrome and neurologic toxicity associated with immune effector cells. *Biol Blood Marrow Transplant.* 2019;25(4):625–638.
22. Stunnenberg HG, Hirst M; International Human Epigenome Consortium. The International Human Epigenome Consortium: a blueprint for scientific collaboration and discovery. *Cell.* 2016;167(5):1145–1149.
23. Xu Y, Zhang M, Ramos CA, et al. Closely related T-memory stem cells correlate with in vivo expansion of CAR.CD19-T cells and are preserved by IL-7 and IL-15. *Blood.* 2014;123(24):3750–3759.
24. Singh N, Perazzelli J, Grupp SA, Barrett DM. Early memory phenotypes drive T cell proliferation in patients with pediatric malignancies. *Sci Transl Med.* 2016;8(320):320ra3.
25. Sadelain M, Rivière I, Riddell S. Therapeutic T cell engineering. *Nature.* 2017;545(7655):423–431.
26. Gattinoni L, Klebanoff CA, Restifo NP. Paths to stemness: building the ultimate antitumour T cell. *Nat Rev Cancer.* 2012;12(10):671–684.
27. Deng Q, Han G, Puebla-Osorio N, et al. Characteristics of anti-CD19 CAR T cell infusion products associated with efficacy and toxicity in patients with large B cell lymphomas. *Nat Med.* 2020;26(12):1878–1887.

28. Iorio F, Knijnenburg TA, Vis DJ, et al. A landscape of pharmacogenomic interactions in cancer. *Cell*. 2016;166(3):740–754.

29. Murtha M, Esteller M. Extraordinary cancer epigenomics: thinking outside the classical coding and promoter box. *Trends Cancer*. 2016;2(10):572–584.

30. Nagel S, Pommerenke C, Meyer C, Kaufmann M, MacLeod RAF, Drexler HG. Identification of a tumor suppressor network in T-cell leukemia. *Leuk Lymphoma*. 2017;58(9):2196–2207.

31. D'Andrea A, Gritti I, Nicoli P, et al. The mitochondrial translation machinery as a therapeutic target in Myc-driven lymphomas. *Oncotarget*. 2016;7(45):72415–72430.

32. Donati G, Brighenti E, Vici M, et al. Selective inhibition of rRNA transcription downregulates E2F-1: a new p53-independent mechanism linking cell growth to cell proliferation. *J Cell Sci*. 2011;124(pt 17):3017–3028.

33. Ji Z, Fan Z, Zhang Y, et al. Thiamine deficiency promotes T cell infiltration in experimental autoimmune encephalomyelitis: the involvement of CCL2. *J Immunol*. 2014;193(5):2157–2167.

34. Li X, Yang B, Wang L, Chen L, Luo X, Liu L. SPAG6 regulates cell apoptosis through the TRAIL signal pathway in myelodysplastic syndromes. *Oncol Rep*. 2017;37(5):2839–2846.

35. Holthof LC, Stikvoort A, van der Horst HJ, et al. Bone marrow mesenchymal stromal cell-mediated resistance in multiple myeloma against NK cells can be overcome by introduction of CD38-CAR or TRAIL-variant. *Hemasphere*. 2021;5(5):e561.

36. Weber EW, Parker KR, Sotillo E, et al. Transient rest restores functionality in exhausted CAR-T cells through epigenetic remodeling. *Science*. 2021;372(6537):eaba1786.

37. Sharma P, Hu-Lieskovan S, Wargo JA, Ribas A. Primary, adaptive, and acquired resistance to cancer immunotherapy. *Cell*. 2017;168(4):707–723.

38. Wang W, Fasolino M, Cattau B, et al. Joint profiling of chromatin accessibility and CAR-T integration site analysis at population and single-cell levels. *Proc Natl Acad Sci U S A*. 2020;117(10):5442–5452.

39. Parker KR, Migliorini D, Perkey E, et al. Single-cell analyses identify brain mural cells expressing CD19 as potential off-tumor targets for CAR-T immunotherapies. *Cell*. 2020;183(1):126–142.e17.

40. Hunter BD, Jacobson CA. CAR T-cell associated neurotoxicity: mechanisms, clinicopathologic correlates, and future directions. *J Natl Cancer Inst*. 2019;111(7):646–654.